On the origin of N in galaxies with galaxy evolution models

Fiorenzo Vincenzo and Chiaki Kobayashi

Centre for Astrophysics Research, University of Hertfordshire
College Lane, AL10 9AB, Hatfield, United Kingdom
emails: f.vincenzo@herts.ac.uk, c.kobayashi@herts.ac.uk

Abstract. Nitrogen is among the most abundant chemical elements in the cosmos, and asymptotic giant branch (AGB) stars are fundamental nucleosynthetic sources of N in galaxies. In this work, we show how the observed N/O versus O/H chemical abundance diagram, both in extragalactic systems and in our own Galaxy, can be used to constrain the nucleosynthetic origin of N in the cosmos. In particular, we review the results of our studies with chemical evolution models, embedded in full cosmological chemodynamical simulations.

Keywords. galaxies: abundances, galaxies: evolution, ISM: abundances, hydrodynamics, stars: abundances

In Fig. 1, we show the observed N/O–O/H chemical abundance diagram as observed in a sample of Milky Way (MW) thin and thick disc stars, and in a sample of MW open clusters Magrini *et al.* (2018), in unresolved star-forming regions within a sample of nearby disc galaxies as observed by the Sloan Digital Sky Survey IV Mapping Nearby Galaxies at Apache Point Observatory survey (MaNGA) Belfiore *et al.* (2017), in the HII regions of a sample of nearby spiral and irregular galaxies by Pilyugin *et al.* (2010), and nearby dwarf galaxies (Izotov *et al.* 2012; James *et al.* 2015; Berg *et al.* 2016; grey triangles with the error bars).

Interestingly, in Fig. 1, the observed stellar N/O–O/H diagram in the Galaxy qualitatively agrees with the observed gas-phase N/O–O/H diagram of the MaNGA survey, which collects chemical abundance measurements from a representative sample of 550 star-forming disc galaxies, with total stellar mass in the range $9.0 \leqslant \log(M_\star/\mathrm{M}_\odot) \leqslant 11.5$ dex. The offset in O/H between Belfiore *et al.* (2017) and Pilyugin *et al.* (2010) is because of the different assumed calibrations to measure the gas metallicity from the strong emission lines; in particular, Belfiore *et al.* (2017) assume as fiducial the calibration of Maiolino *et al.* (2008). Despite the large uncertainty in the assumed metallicity calibrations, the observations agree that N/O steeply increases when moving towards high O/H. At very low metallicity, N/O tends to remain flat around a mean value of ~ -1.5 dex, with a large scatter (see also the early work of Matteucci 1986).

The observed behaviour of N/O as a function of O/H depends on how N is produced by stars of different mass and metallicity. From a nucleosynthesis point of view, N is mostly produced as a *secondary* element; in particular, stars of larger metallicities produce – on average – larger amounts of N. The secondary N is synthesised during the CNO cycle of H-burning, at the expenses of the C and O nuclei already present in the gas mixture from which the star originated (see, for more details, Henry *et al.* 2000; Chiappini *et al.* 2005; Mollá *et al.* 2006; Gavilán *et al.* 2006; Vincenzo *et al.* 2016).

At very low metallicity, where massive stars are predominant in the chemical enrichment process, and the secondary N component is minimal, we observe a plateau of N/O
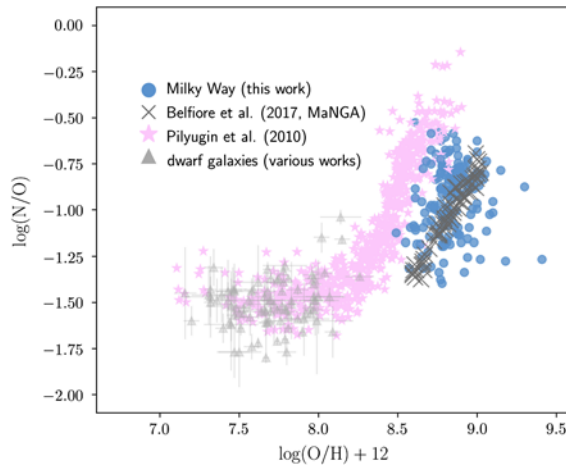
Figure 1. We compare the observed N/O–O/H relation in the MW stars and open cluster Magrini *et al.* (2018), in a sample of MaNGA survey galaxies (Belfiore *et al.* 2017; grey crosses), in the HII regions of nearby spiral and irregular galaxies (Pilyugin *et al.* 2010; pink stars), and in nearby dwarf galaxies (Izotov *et al.* 2012; James *et al.* 2015; Berg *et al.* 2016; grey triangles with the error bars).

versus O/H; to reproduce this plateau, an additional mechanism has been invoked by chemical evolution models of galaxies, requiring that N is mostly produced as a *primary* element by very metal-poor massive stars, namely its nucleosynthesis yields do not depend on the initial metal content of the stars (Matteucci 1986; Chiappini *et al.* 2005). Since stellar evolution models of massive stars typically fail in predicting the necessary amount of primary N to reproduce the observations, chemical evolution models assumed in the past a fixed, artificial amount of primary N from very metal-poor massive stars to reproduce N/O at very low metallicity.

We remark on the fact that also AGB stars can produce primary N during the so-called third dredge-up, when it occurs in conjunction with the hot-bottom burning, if nuclear burning at the base of the convective envelope is efficient (Renzini & Voli 1981; Ventura *et al.* 2013).

Cosmological chemodynamical simulations are nowadays among the best tools to study how chemical elements are produced within galaxies, to reconstruct also the spatial distribution of the chemical elements as a function of time within different galaxy environments. Our simulation code includes the main stellar nucleosynthetic sources in the cosmos (core-collapse and Type Ia supernovae, hypernovae, asymptotic giant branch stars, and stellar winds from stars of all masses and metallicities), and it is based on an updated version of the GADGET 3 code (Springel *et al.* 2001; Springel 2005; Kobayashi, 2004; Kobayashi *et al.* 2007; Kobayashi & Nakasato 2011).

In Figs. 2 and 3, we present the results of the cosmological chemodynamical simulation developed by Vincenzo & Kobayashi (2018a,b), including also the effect of failed supernovae (Kobayashi *et al.* in prep.). In Fig. 2 we show how the gas-phase N/O versus O/H abundance patterns vary within ten reference simulated galaxies, which have been selected because of their different star formation histories (SFHs); in particular, from galaxy 0 to galaxy 10, the SFH is concentrated towards later and later epochs (see Vincenzo & Kobayashi 2018b). The blue points in 2 correspond to the predictions of our simulation, while the pink crosses correspond to the MaNGA data of Belfiore *et al.* (2017); we also show the average observed relation as derived by Dopita *et al.* (2016; solid grey line). The black points with the error bars correspond to the predicted average N/O and O/H which have been computed by dividing our simulated galaxies in many
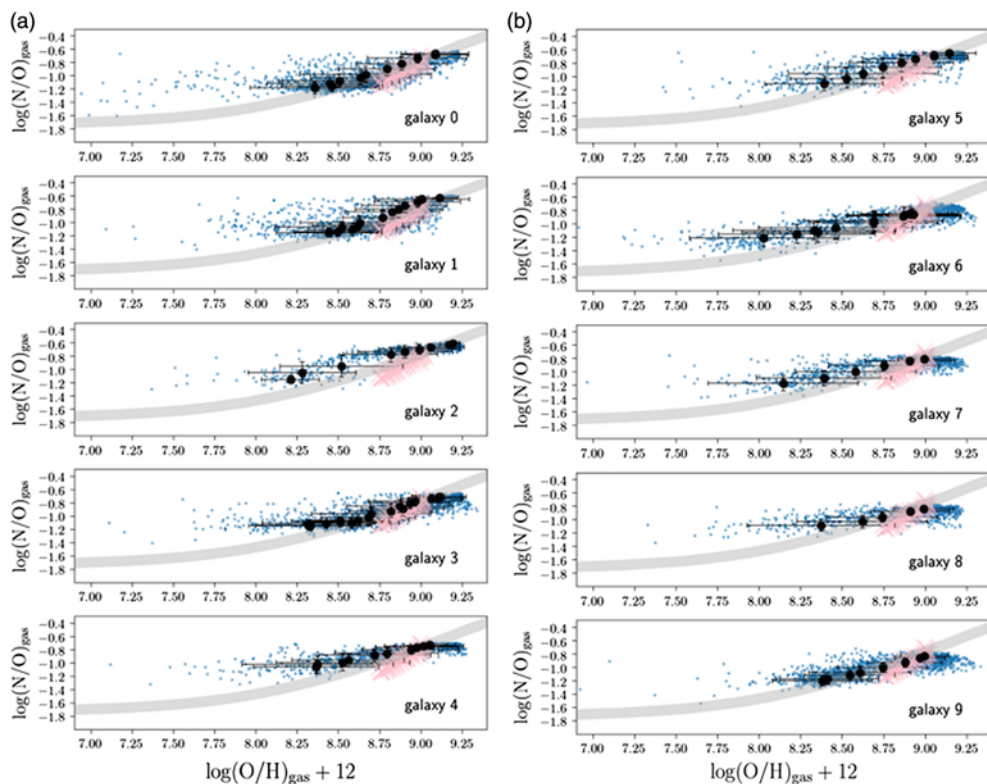
Figure 2. The predicted gas-phase N/O–O/H relation within our ten reference disc galaxies, where each blue point corresponds to a gas particle, and the black points with error bars have been computed, firstly by dividing in different annuli the simulated galaxies, and then by computing the average N/O and O/H within each annulus; the pink crosses correspond to the MaNGA survey data of Belfiore *et al.* (2017), while the solid grey line to the average observed relation of Dopita *et al.* (2016).
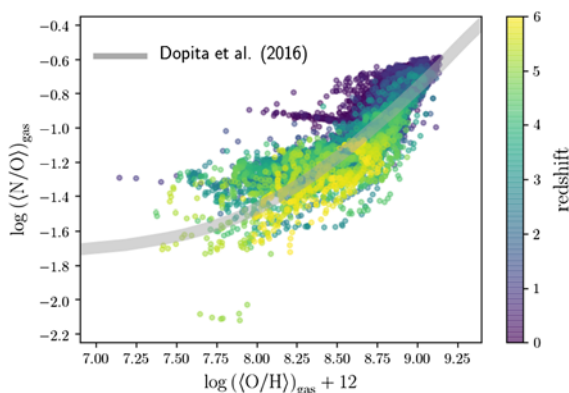

Figure 3. The predicted N/O–O/H relation, where the abundances correspond to SFR-weighted averages in the gas-phase of all 33 disc galaxies in our sample, which – in this case – are unresolved. See Vincenzo & Kobayashi (2018b) for more details about Figs. 2 and 3.

concentric annuli. We predict that – when we are able to spatially resolve galaxies – their N/O–O/H diagram tend to follow at the present time an average universal relation, which does not depend on the galaxy SFH, simply because the nucleosynthesis of N is universal, and it strictly depends – in the relatively high metallicity regime – on the metallicity of the stars. The trend of N/O versus O/H in Fig. 2 reflects chemical abundance gradients in our simulated galaxies, where the innermost metal-rich regions have higher N/O ratios than the outermost metal-poor regions.

In Fig. 3, we show how the average gas-phase N/O within 33 star-forming disc galaxies in our simulation volume vary as functions of the average gas-phase O/H. The colour-coding in the figure corresponds to the redshift. We predict that, even in the case of unresolved galaxies, their average N/O ratios tend to obey the same observed average relation as in the case of resolved galaxies. In this case, the relation between the average N/O and O/H is the consequence of a mass-metallicity relation that our simulated galaxies obey – on average – as they evolve across cosmic times, with the most massive galaxies having typically higher O/H (and hence higher N/O because of the main secondary origin of N) than the least massive systems.

Coming back to the original discussion on Fig. 1, our chemodynamical simulations have been able to predict and explain the reason why the gas-phase abundances of N/O versus O/H from the MaNGA survey are consistent with the abundances of the MW stars and open clusters. In conclusion, to respond also to the question of Letizia Stanghellini at the end of our presentation, we note that the stellar abundances in the MW stars can be used in the future to identify the best metallicity calibration for strong emission line diagnostics, as suggested in the original draft of Magrini *et al.* (2018).

References

Belfiore, F., Maiolino, R., Tremonti, C., *et al.* 2017, *MNRAS*, 469, 151
Berg, D. A., Skillman, E. D., Henry, R. B. C., Erb, D. K., & Carigi L., 2016, *ApJ*, 827, 126
Chiappini, C., Matteucci, F., & Ballero, S. K. 2005, *A&A*, 437, 429
Dopita, M. A., Kewley, L. J., Sutherland, R. S., & Nicholls D. C., 2016, *APSS*, 361, 61
Gavilán, M., Mollá, M., & Buell, J. F. 2006, *A&A*, 450, 509
Henry, R. B. C., Edmunds, M. G., & Köppen, J. 2000, *ApJ*, 541, 660
Izotov, Y. I., Thuan, T. X., & Guseva, N. G., 2012, *A&A*, 546, A122
Iwamoto, K., Brachwitz, F., Nomoto, K., *et al.* 1999, *ApJS*, 125, 439
James, B. L., Koposov, S., Stark D. P., *et al.*, 2015, *MNRAS*, 448, 2687
Karakas, A. I. 2010, *MNRAS*, 403, 1413
Kobayashi, C. 2004, *MNRAS*, 347, 740
Kobayashi, C., Springel, V., & White, S. D. M., 2007, *MNRAS*, 376, 1465
Kobayashi, C., & Nakasato, N., 2011, *ApJ*, 729, 16
Kroupa, P., Tout, C. A., & Gilmore, G., 1993, *MNRAS*, 262, 545
Magrini, L., Vincenzo, F., Randich, S., *et al.* 2018, *A&A*, 618, A102
Maiolino, R., Nagao, T., Grazian, A., *et al.* 2008, *ApJ*, 488, 463
Matteucci, F. 1986, *MNRAS*, 221, 911
Mollá, M., Vílchez, J. M., Gavilán, M., & Díaz, A. I. 2006, *MNRAS*, 372, 1069
Nomoto, K., Kobayashi, C., & Tominaga, N. 2013, *ARA&A*, 51, 457
Pilyugin, L. S., Vílchez, J. M., & Thuan, T. X. 2010, *ApJ*, 720, 1738
Renzini, A., & Voli, M. 1981, *A&A*, 94, 175
Springel, V., Yoshida, N., & White, S. D. M. 2001, *NA*, 6, 79
Springel, V. 2005, *MNRAS*, 364, 1105
Totani, T., Morokuma, T., Oda, T., Doi, M., & Yasuda, N. 2008, *PASJ*, 60, 1327
Ventura, P., Di Criscienzo, M., Carini, R., & D'Antona, F. 2013, *MNRAS*, 431, 3642
Vincenzo, F., Belfiore, F., Maiolino, R., Matteucci, F., & Ventura, P. 2016, *MNRAS*, 458, 3466
Vincenzo, F., & Kobayashi, C. 2018a, *A&A*, 610, L16
Vincenzo, F., & Kobayashi, C. 2018b, *MNRAS*, 478, 155